Radiation Noise Reduction using Spread Spectrum for Inductive Power Transfer Systems considering Misalignment of Coils

Keisuke Kusaka, Kent Inoue, Jun-ichi Itoh
Department of Electrical, Electronics and Information Engineering
Nagaoka University of Technology
Nagaoka, Niigata, Japan
kusaka@vos.nagaokaut.ac.jp, k_inoue@stn.nagaokaut.ac.jp, itoh@vos.nagaokaut.ac.jp

***Abstract*—This paper proposes spread spectrum methods to reduce radiation noise caused by an inductive power transfer (IPT) system. A noise reduction method with spread spectrum techniques has been proposed. The proposed noise reduction method randomly changes the output frequency of an inverter within a range of 79-to-90 kHz. Changing the output frequency, the radiation noise is spread in a frequency domain. A previous study has proposed the spread spectrum method with the biased probability distribution, which improves the noise reduction performance. However, the suitable probability distribution has not been clear. This paper proposes two spread spectrum methods with biased probability distributions, which are proportional and inverse proportional to an input impedance of the IPT system. The proposed methods are assessed and compared with the conventional noise reduction method. Considering the input impedance of the IPT system, the radiation noise from the IPT system with or without the coil misalignment is reduced by 13.4 dBμA and 7.0 dBμA in comparison with the constant frequency operation. Moreover, the reduction performance is improved compared to the conventional spread spectrum method.**

Keywords—inductive power transfer; wireless power transfer; radiation noise; EMI; spread spectrum; random carrier

I. INTRODUCTION

Inductive power transfer (IPT) systems for electrical vehicles (EVs) are actively studied [1-7] in recent years. The IPT is expected to improve the convenience of users of EVs when the users charge an onboard battery. Especially, a development of a suppression method of radiation noise from an IPT system for EVs is highly required [8-14] in order to put it to practical use. The radiative emission has to be suppressed because the radiation noise may cause malfunctions of wireless communication systems or electronic equipment placed nearby IPT systems. From a practical application perspective, radiation noise has to be suppressed to respect the regulations, which will be legislated in each area or nations. The regulations in each area or nations will be legislated to be conformed to the guidelines published by CISPR [15]. Ref. [8-11] reduce the radiation noise using magnetic shields and metal shields, which are put nearby the coils. These shields effectively suppress radiation noise because a reluctance of a leakage path of magnetic flux is increased. However, eddy current loss occurs in these shields. As another approach, a noise reduction method using a low-pass filter is used. The low-pass filter is inserted between a primary inverter and a transmitting coil. A cut-off frequency of the low-pass filter has to be set at the frequency between the fundamental frequency and three times the fundamental frequency to reduce the low-order harmonics components of the current. It decreases the efficiency of the IPT system because it will degrade a power factor from the viewpoint of the inverter at the fundamental frequency. In [12], the EMI reduction technique using two-channel IPT system with currents of opposite phase has been proposed. The two set of the coils are placed to cancel out the radiation noise. It is effective to cancel out the radiation noise. However, the two-channel IPT system has poor freedom on the coil placement because it needs four coils.

In [13-14], spread spectrum methods have been proposed. The spread spectrum achieves noise reduction by randomly changing an output frequency of the inverter. Thus, the spread spectrum method does not require additional components such as metal plates, magnetic shields, or additional coils. By selecting the output frequency of the inverter from a biased probability distribution, the effect of spread spectrum is improved in comparison with the spread spectrum with an uniform probability distribution because the IPT system has a frequency dependence at around a resonance frequency. However, the optimum probability distribution is not discussed in [13-14]. In addition, the reduction effect has been tested under the condition that a misalignment of the transmission coils is unconsidered. In order to put it into a practical use, the reduction methods have to be effective even if the misalignment of the coils occurs.

In this paper, novel spread spectrum methods are proposed and assessed. The probability distribution is determined by considering the input impedance of the IPT system at a nominal position in the proposed method. Considering a frequency dependence of the input impedance of the IPT system, the radiation noise is reduced regardless of the misalignment. This paper consists of following sections; first, the regulations for the radiation noise from the IPT system in Japan is explained. Then, two reduction methods using spread spectrum are proposed. Third, the proposed method is

compared to the conventional method considering the misalignment of coils with a 3-kW prototype.

II. Inductive Power Transfer Systems for EVs

A. Regulations of Radiation Noise

Figure 1 shows the guideline of the radiation noise in Japan for the IPT systems toward EVs with a power of 7.7 kW or less [16]. The regulation was legislated in Japan in 2015. Basically, the standard is conformed to the CISPR 11/Group 2/Class B [15]. Note that the allowable limits are converted to the limits with measuring at 10 m according to CISPR/B/587A/INF because CISPR 11/Group 2/Class B requires measuring the noise at 3 m. Moreover, CISPR11 requires measuring the radiation noise with a quasi-peak measuring method.

In the regulation, the frequency band from 79 to 90 kHz has been assigned as the transmission frequency of the IPT systems for EVs. The allowable limits of the radiation noise on the transmission frequency is relaxed from 23.1 dBμA/m to 68.4 dBμA/m at 10 m. In addition, the guideline on the following frequency bands is relaxed by 10 dB from CISPR 11/Group 2/Class B.

- 158 – 180 kHz
- 237 – 270 kHz
- 316 – 360 kHz
- 395 – 450 kHz

In contrast, the regulation within 526.5 to 1606.5 kHz is set at -2.0 dBμA/m because these frequency bands have been assigned to the amplitude modulation (AM) broadcasting. This frequency overlaps with the seventh harmonics. Thus the frequency components and the low-order harmonics have to be suppressed.

B. System configuration

Figure 2 shows the system configuration of the typical IPT system for EVs. A primary coil is buried in the parking, whereas a secondary coil is beneath the bottom of the vehicles. Thus the magnetic coupling between these coils is weak. The compensation circuits such as a series-parallel compensation (S/P), series-series compensation (S/S), parallel-parallel compensation (P/P), or parallel-series compensation (P/S) have been proposed [17] in order to overcome the problems. In addition to the above methods, there are several combinations of connections of capacitors and inductors as the compensation circuits. However, the common concept of the compensation circuit is the improvement of the power factor from the inverter and the induced voltage on the secondary coils.

Besides, a buck or boost converter is typically connected in order to maintain the transmission efficiency regardless of the change of input voltage [18].

In this paper, the series–series compensation (S/S) is used in order to cancel out the reactance caused by the leakage inductance. The current on the primary coil and the secondary coil are expressed as (1) and (2) using the equivalent load resistance $R_{eq.}$

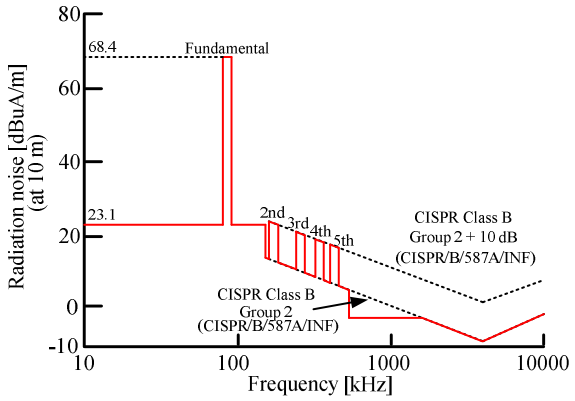

Fig. 1. Guideline of radiation noise for 7.7-kW or less IPT system for EVs in Japan.

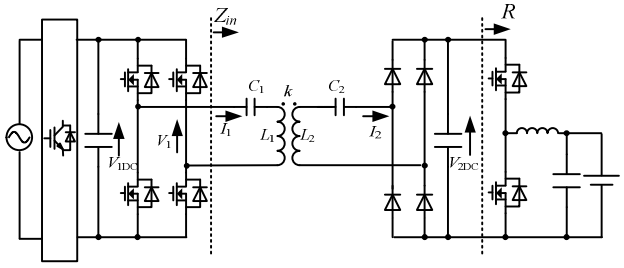

Fig. 2. System configuration example of IPT system for EVs.

$$\dot{I}_1 = \frac{r_2 + R_{eq} + j\left(\omega L_2 - \frac{1}{\omega C_2}\right)}{\left\{r_1 + j\left(\omega L_1 - \frac{1}{\omega C_1}\right)\right\}\left\{r_2 + R_{eq} + j\left(\omega L_2 - \frac{1}{\omega C_2}\right)\right\} + \omega^2 L_m^2}\dot{V}_1 \quad (1)$$

$$\dot{I}_2 = \frac{j\omega L_m}{\left\{r_1 + j\left(\omega L_1 - \frac{1}{\omega C_1}\right)\right\}\left\{r_2 + R_{eq} + j\left(\omega L_2 - \frac{1}{\omega C_2}\right)\right\} + \omega^2 L_m^2}\dot{V}_1 \quad (2)$$

Note L_1 is the primary inductance, L_2 is the secondary inductance, L_m is the mutual inductance, r_1 is the series resistance of the primary winding, r_2 is the series resistance of the secondary winding, C_1 is the primary compensation capacitor, C_2 is the secondary compensation capacitor, ω is the angular frequency of the power supply, and V_1 is the fundamental component of the output voltage of the inverter.

The relationship between the primary voltage V_1 and primary DC-voltage when the inverter is operated with a square wave output voltage is expressed by

$$V_1 = \frac{2\sqrt{2}}{\pi}V_{1DC} \quad (3).$$

The equivalent AC load resistance is calculated by (4) using the analysis given in [19].

$$R_{eq} = \frac{8}{\pi^2}\frac{V_{2DC}^2}{P_2} = \frac{8}{\pi^2}R \qquad (4)$$

where V_{2DC} is the secondary DC voltage and P_2 is the output power.

The compensation capacitors are designed to cancel out the reactance at the transmitting frequency. Thus, the capacitance value of the compensation capacitors should be designed according to

$$C_1 = \frac{1}{L_1\omega^2} \qquad (5),$$

$$C_2 = \frac{1}{L_2\omega^2} \qquad (6).$$

Substituting (5) and (6) to (1), the primary current with the compensation is expressed by

$$\dot{I}_1 = \frac{r_2 + R_{eq}}{r_1(r_2 + R_{eq}) + \omega^2 L_m^2}\dot{V}_1 \qquad (7)$$

under the resonance conditions.

The power factor from the output of the power supply is unity owing to the compensation capacitors.

III. Noise Reduction Methods

Radiation noise is caused by the currents, which flow in the transmission coils. In [13-14], a noise reduction method using the spread spectrum technique has been proposed. The output frequency of the primary inverter is changed within a range of 79-to-90 kHz at every period, which is allowable frequency band for IPT system shown in Fig. 1. The output frequency is randomly selected. Due to this operation, the radiation noise will be spread in a frequency domain. Moreover, Ref. [14] proposed to select the switching frequency with the probability distribution, which has a bias but not the uniform discrete probability distribution. The probability distribution proposed in [14] is proportional to the combined impedance of the primary inductance and the primary capacitance. Ref. [14] experimentally assessed the effect of the biased probability distribution. However, the adequate probability distribution to suppress the noise is not discussed. In this paper, two spread spectrum methods are proposed and experimentally compared to the conventional spread spectrum method.

Figure 3 explains the generation method of pseudo-random numbers. For all of the spread spectrum methods tested in this paper, pseudo-random numbers are used in order to select the output frequency in random. The pseudo random numbers are generated using a maximal length sequence (M-sequence) [20-21] on a DSP (Digital signal processor). The M-sequence based generation algorithm of the pseudo random numbers is suitable to implement to the DSP because it does not require much calculation.

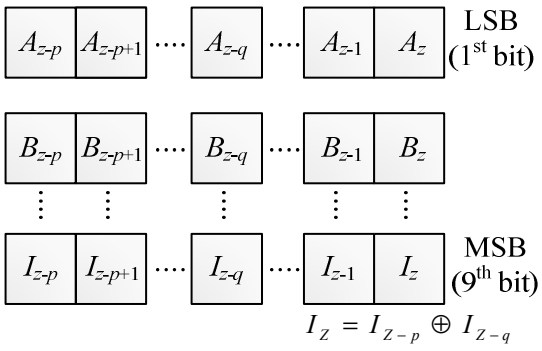

Fig. 3. 9-bit pseudo random number generation based on a M-sequence.

A random number based on the M-sequence is generated by

$$I_z = I_{z-p} \oplus I_{z-q} \qquad (8),$$

where I_{z-p} and I_{z-q} are the present value I_z delayed by p and q periods, respectively ($p > q$). The present value is an Exclusive-Or of the I_{Z-p} and I_{Z-q}. In this experiments, $p = 9$, $q = 1$ are used. Moreover, a bit number of the pseudo-random number is nine.

A. Conventional Method (Probability distribution proportional to combined impedance of LC)

Figure 4(a) shows the probability distribution, which is used as the conventional method. The output frequency is selected according to the Table I (a). Table I indicates the random numbers, which are generated by M-sequence. The conventional method uses the biased discrete probability distribution for the spread spectrum technique. The probability distribution is determined proportionally to a combined impedance of the transmission coil and the primary compensation capacitor. The frequency span among each frequency is limited to 650 Hz owing to a clock frequency of the FPGA (Field-programmable gate array), which is used to generate the carrier for the inverter.

The combined impedance is expressed as (9) when an equivalent series resistance of the primary coils can be ignored.

$$\dot{Z}_{LC} = j\omega L - j\frac{1}{\omega C} \qquad (9)$$

B. Proposed Method I (Probability distribution proportional to Z_{in}

In this paper, two spread spectrum methods are proposed. Figure 4(b) shows the first proposed probability distribution. The first proposed method uses biased probability distribution, which is proportional to an absolute value of an input impedance $|Z_{in}|$. The output frequency is selected according to

Table I (b) using the pseudo-random numbers, which are generated by M-sequence.

From (1), the absolute value of the primary current is calculated by (10) using (9).

$$\left|\dot{I}_1\right| = \frac{\sqrt{R_{eq}^2\omega^4 L_m^4 + \left|\dot{Z}_{LC}^2\right|\left(\omega^2 L_m^2 - \left|\dot{Z}_{LC}^2\right| - R_{eq}^2\right)^2}}{\left(\omega^2 L_m^2 - \left|\dot{Z}_{LC}^2\right|\right)^2 + R_{eq}^2\left|\dot{Z}_{LC}^2\right|}\left|\dot{V}_1\right| \tag{10}$$

From (10), the input impedance $|Z_{in}|$ is derived as (11) when the optimal load for the maximum efficiency is connected to the load.

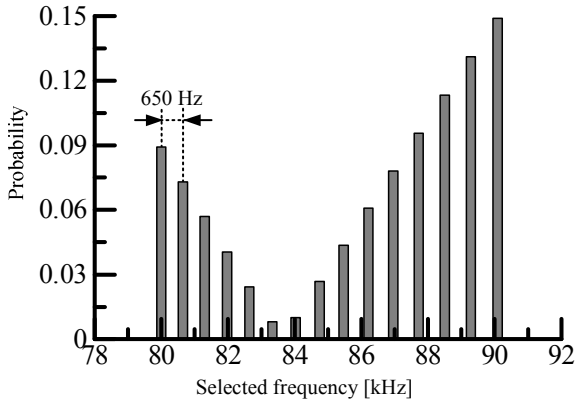

(a) In proportion to combined impedance of inductor and capacitor Z_{LC} (conventional)

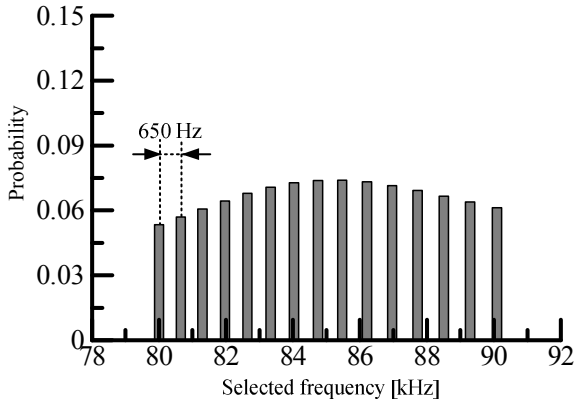

(b) In proportion to input impedance Z_{in}

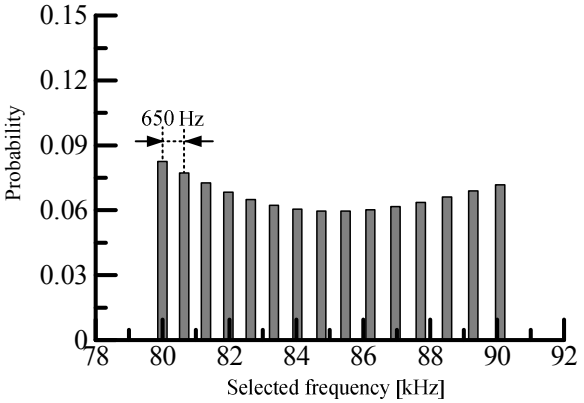

(c) In inverse proportion to input impedance Z_{in}

Fig. 4. Probability distributions.

TABLE I. ASSIGNMENT OF OUTPUT FREQUENCY.

(a) In proportion to combined impedance of inductor and capacitor Z_{LC} (conventional)

	Psuedo random numbers	Frequency [kHz]		Psuedo random numbers	Frequency [kHz]
0	000000000	80.00	168	010101000	85.47
⋮	⋮	80.00	⋮	⋮	85.47
45	000101101	80.00	189	010111101	85.47
46	000101110	80.65	190	010111110	86.21
⋮	⋮	80.65	⋮	⋮	86.21
82	001010010	80.65	220	011011100	86.21
83	001010011	81.30	221	011011101	86.96
⋮	⋮	81.30	⋮	⋮	86.96
111	001101111	81.30	260	100000100	86.96
112	001110000	81.97	261	100000101	87.72
⋮	⋮	81.97	⋮	⋮	87.72
132	010000100	81.97	309	100110101	87.72
133	010000101	82.64	310	100110110	88.50
⋮	⋮	82.64	⋮	⋮	88.50
144	010010000	82.64	367	101101111	88.50
145	010010001	83.33	368	101110000	89.29
⋮	⋮	83.33	⋮	⋮	89.29
148	010010100	83.33	434	110110010	89.29
149	010010101	84.03	435	110110011	90.09
⋮	⋮	84.03	⋮	⋮	90.09
153	010011001	84.03	510	111111110	90.09
154	010011010	84.75	511	111111111	-
⋮	⋮	84.75			
167	010100111	84.75			

(b) In proportion to input impedance Z_{in}

	Psuedo random number	Frequency [kHz]		Psuedo random numbers	Frequency [kHz]
0	000000000	80.00	266	100001010	85.47
⋮	⋮	80.00	⋮	⋮	85.47
26	000011010	80.00	303	100101111	85.47
27	000011011	80.65	304	100110000	86.21
⋮	⋮	80.65	⋮	⋮	86.21
55	000110111	80.65	340	101010100	86.21
56	000111000	81.30	341	101010101	86.96
⋮	⋮	81.30	⋮	⋮	86.96
86	001010110	81.30	377	101111001	86.96
87	001010111	81.97	378	101111010	87.72
⋮	⋮	81.97	⋮	⋮	87.72
119	001110111	81.97	412	110011100	87.72
120	001111000	82.64	413	110011101	88.50
⋮	⋮	82.64	⋮	⋮	88.50
154	010011010	82.64	446	110111110	88.50
155	010011011	83.33	447	110111111	89.29
⋮	⋮	83.33	⋮	⋮	89.29
190	010111110	83.33	479	111011111	89.29
191	010111111	84.03	480	111100000	90.09
⋮	⋮	84.03	⋮	⋮	90.09
227	011100011	84.03	510	111111110	90.09
228	011100100	84.75	511	111111111	-
⋮	⋮	84.75			
265	100001001	84.75			

(c) In inverse proportion to input impedance Z_{in}

	Psuedo random numbers	Frequency [kHz]		Psuedo random numbers	Frequency [kHz]
0	000000000	80.00	279	100010111	85.47
⋮	⋮	80.00	⋮	⋮	85.47
41	000101001	80.00	308	100110100	85.47
42	000101010	80.65	309	100110101	86.21
⋮	⋮	80.65	⋮	⋮	86.21
80	001010000	80.65	339	101010011	86.21
81	001010001	81.30	340	101010100	86.96
⋮	⋮	81.30	⋮	⋮	86.96
117	001110101	81.30	371	101110011	86.96
118	001110110	81.97	372	101110100	87.72
⋮	⋮	81.97	⋮	⋮	87.72
152	010011000	81.97	403	110010011	87.72
153	010011001	82.64	404	110010100	88.50
⋮	⋮	82.64	⋮	⋮	88.50
185	010111001	82.64	437	110110101	88.50
186	010111010	83.33	438	110110110	89.29
⋮	⋮	83.33	⋮	⋮	89.29
217	011011001	83.33	472	111011000	89.29
218	011011010	84.03	473	111011001	90.09
⋮	⋮	84.03	⋮	⋮	90.09
248	011111000	84.03	509	111111101	90.09
249	011111001	84.75	510	111111110	-
⋮	⋮	84.75	511	111111111	-
278	100010110	84.75			

$$\left|\dot{Z}_{in}\right| = \frac{\left(\omega^2 L_m^2 - \left|\dot{Z}_{LC}^2\right|\right)^2 + R_{eq}^2 \left|\dot{Z}_{LC}^2\right|}{\sqrt{R_{eq}^2 \omega^4 L_m^4 + \left|\dot{Z}_{LC}^2\right|\left(\omega^2 L_m^2 - \left|\dot{Z}_{LC}^2\right| - R_{eq}^2\right)^2}} \tag{11}$$

Figure 5 shows the measurement result and the calculation result of the input impedance at the nominal position. It confirms that the calculation result shows good agreement with the measurement result.

C. *Proposed Method II (Probability distribution inverse proportional to Z_{in})*

Figure 4(c) shows the probability distribution for the second proposed method. The probability distribution is inverse proportional to the input impedance Z_{in}. The input impedance can be calculated by (11) using the parameters at nominal position. The output frequency is selected according to Table I (c) using the pseudo-random numbers.

IV. Experiments

A. *Experimental Setup*

Table II shows the specifications of the experimental setup. In these experiments, a 400-V DC voltage source is directly connected to the primary inverter for simplicity. Moreover, a resistance load is directly connected to the output of the full-bridge rectifier.

Figure 6 shows the transmission coils of the prototype. A solenoid type is used because the solenoid type typically has higher magnetic coupling in comparison with a circular coil in return for large radiation noise.

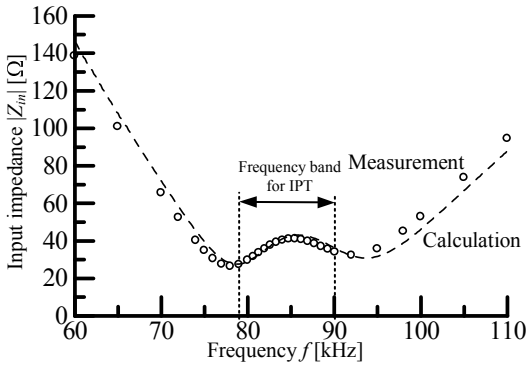

Fig. 5. Input Impedance of the IPT system.

TABLE II. Specification of IPT system.

	Symbol	Value	Note
Input DC voltage	V_{DC1}	400 V	
Transmission distance	l	150 mm	(nominal position)
Coupling coefficient	k	0.2	@150 mm (nominal position)
		0.3	@100 mm
Primary inductance	L_1	392 uH	@150 mm (nominal position)
		422 uH	@100 mm
Secondary inductance	L_2	401 uH	@150 mm (nominal position)
		428 uH	@100 mm
Primary capacitance	C_1	8.9 nF	
Secondary capacitance	C_2	8.8 nF	
Ferrite plates		PC40 (TDK Corporation)	
MOSFETs		SCH2080KEC (ROHM Co., Ltd.)	
Diodes		SCS220AE (ROHM Co., Ltd.)	

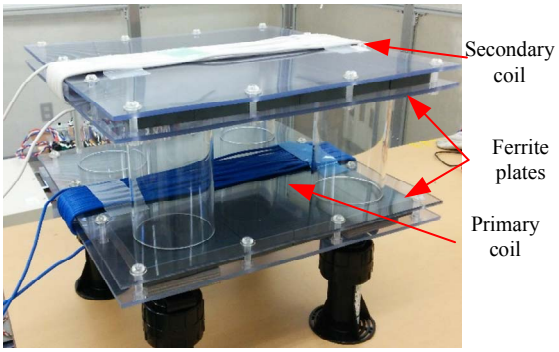

Fig. 6. Primary and Secondary coils of prototype.

When the coils are placed in the nominal position, magnetic coupling is k = 0.2. Assuming the change of transmission distance from 150 to 100 mm, a magnetic coupling is increased from 0.2 to 0.3. The change of the transmission distance also causes a change of the primary and the secondary inductance. It will cause the difference between the resonance frequency and the transmitting frequency because the resonance capacitor is designed to resonate with the inductance at the nominal transmission distance.

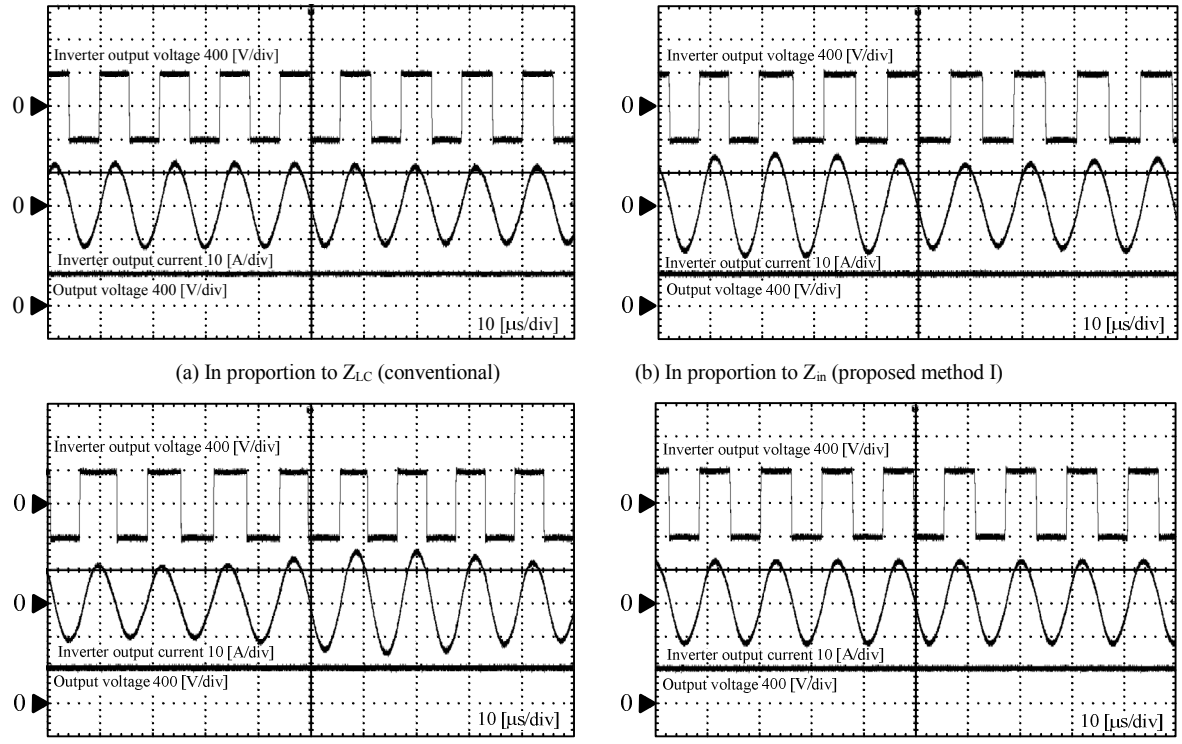

(a) In proportion to Z_{LC} (conventional) (b) In proportion to Z_{in} (proposed method I)

(c) In inverse proportion to Z_{in} (proposed method II) (d) Constant frequency

Fig. 7. Operation waveforms without coil misalignment (3 kW) where Z_{in} is the input impedance and Z_{LC} is the combined impedance of the inductor and capacitor.

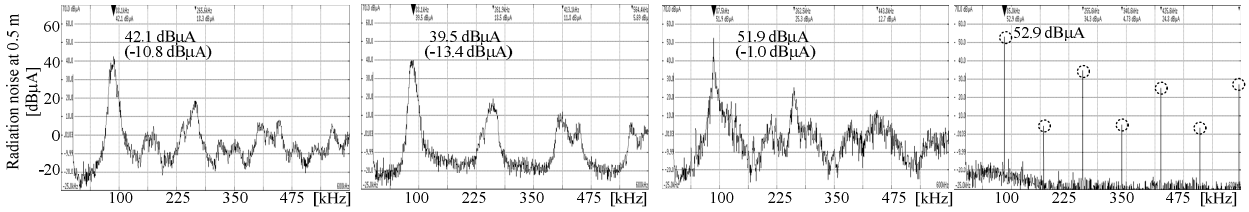

(a) In proportion to Z_{LC} (conv.) (b) In proportion to Z_{in} (proposed) (c) In inverse proportion to Z_{in} (proposed) (d) Constant frequency

Fig. 8. Radiation noise without misalignment when output power is 3 kW where Z_{in} is the input impedance and Z_{LC} is the combined impedance of the inductor and capacitor.

B. Operation without coil misalignment

Figure 7 shows the waveforms with a 3.3-kW IPT system. Fig. 7 (a) is operation waveforms with the conventional spread spectrum method. The probability distribution is biased in proportion to the combined impedance Z_{LC}. Figs. 7 (b) and (c) are the waveforms with the proposed probability distributions. The probability distributions are in proportion and inverse proportion to the input impedance Z_{in}. Fig. 7 (d) is the waveforms when the inverter is operated at a constant frequency (84.75 kHz). In Figs. 7 (a), (b) and (c), the output frequency is changed within the range or 79-to-90 kHz at every period according to the probability distribution. Due to the change of an inverter output frequency, the amplitude of the inverter output current i_1 changes.

Figure 8 shows the spectrum of the radiation emission observed at 0.5 m from the edge of coils. The transmission

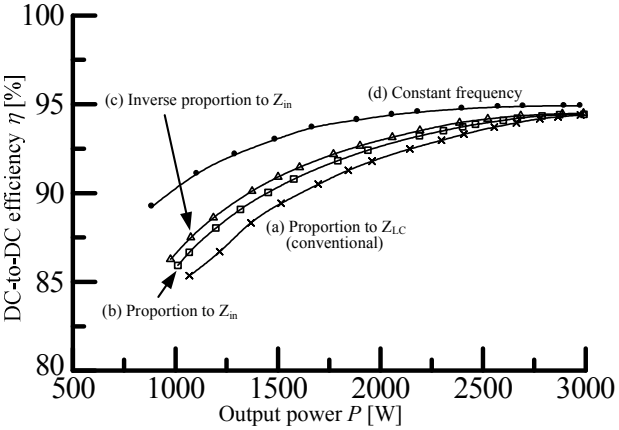

Fig. 9. DC-to-DC efficiency withtout coil misalignment.

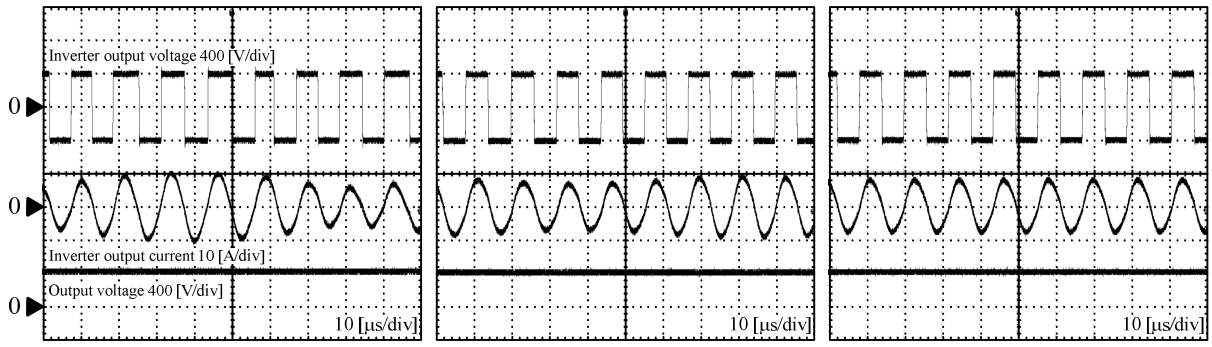

(a) In proportion to Z_{LC} (conventional) (b) Proportion to Z_{in} (proposed method I) (c) Constant frequency

Fig. 10. Operation waveforms with a coil misalignment (1.9 kW) where Z_{in} is the input impedance and Z_{LC} is the combined impedance of the inductor and capacitor.

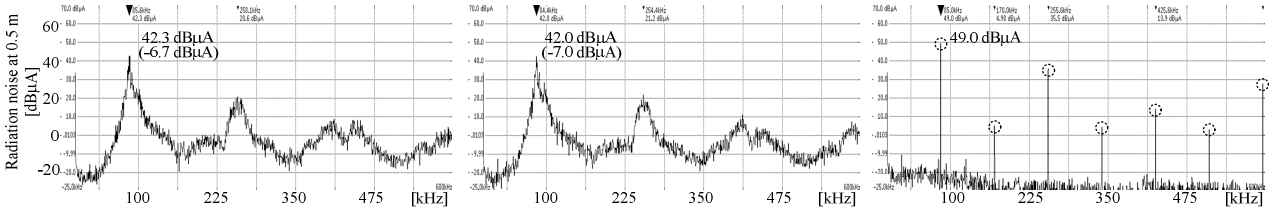

(a) In proportion to Z_{LC} (conv.) (b) In proportion to Z_{in} (proposed) (c) Constant frequency

Fig. 11. Radiation noise with a coil misalignment (1.9 kW) where Z_{in} is the input impedance and Z_{LC} is the combined impedance of the inductor and capacitor.

coils are placed in the nominal position in this experiment. When the output frequency of the inverter is constant (Fig. 7 (d)), the sharp fundamental and low-order harmonic components are observed. Using the biased distribution, which is in proportion to Z_{LC}, a maximum value at the fundamental frequency is suppressed by 10.8 dBμA in comparison with the constant frequency operation. The first proposed method using proportional distribution to Z_{in} suppresses the noise by 13.4 dBμA. In contrast, the second proposed method using inverse proportional distribution suppresses the noise by 1.0 dBμA. It can be understood from these results, the first proposed method using the probability distribution, which is proportional to the input impedance is the most effective to suppress the noise.

Fig. 9 shows the experimental results of the DC-to-DC efficiencies without coil misalignment. In this paper, the efficiency from DC input to DC output is evaluated. The maximum efficiency is 94.9% at an output power of 3.0 kW when the inverter is operated at a constant frequency. The efficiency of the first proposed method, which uses a proportional distribution to Z_{in}, is decreased from 94.9% to 94.4% with at the same output power of 3.0 kW. It is confirmed that the effect of the proposed noise reduction method on the efficiency is small enough to be negligible at the rated power. Furthermore, the efficiency of the first proposed method is higher than the conventional spread spectrum method in the light-load region.

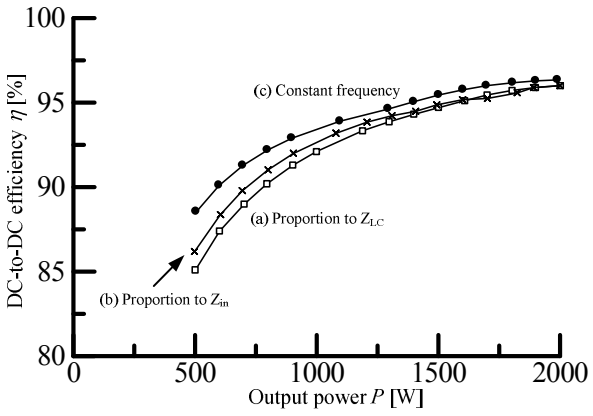

Fig. 12. DC-to-DC efficiency with a coil misalignment.

C. Operation with coil misalignment

Figure 10 shows the operation waveforms of the IPT systems with a coil misalignment. The transmission distance is changed from the nominal distance of 150 mm to 100 mm. Due to the change of the transmission distance, the magnetic coupling changes from 0.2 to 0.3. The output power is limited to 1.9 kW owing to a mismatch of resonance parameters. The proposed method I, which uses the probability distribution being in proportion to $|Z_{in}|$, is compared to the constant operation and conventional spread spectrum method. Regardless to the coil misalignment, the power can still be supplied from the primary to the secondary side.

Figure 11 shows the radiation noise with the coil misalignment. The peak of the radiation noise on the fundamental frequency is suppressed from 49.0 dBμA (constant frequency) to 42.3 dBμA (the conventional method) and 42.0 dBμA (the proposed method). The difference in the performance of the proposed method and the conventional method is small. Besides, when the coil misalignment occurs, the reduction performance degrades in comparison with the operation without the coil misalignment. It is confirmed that, however, the spread spectrum is also effective to reduce the radiation noise even if the coil misalignment occurs.

Figure 12 shows the efficiency characteristics of the IPT system with the coil misalignment. The maximum efficiencies are 96.3%, 96.0%, and 96.0% at the rated power when the inverter is operated with the constant frequency operation and two noise reduction methods. The use of the spread spectrum decreases the DC-to-DC efficiency, however, the decrease in the efficiency is only 0.3%. It is confirmed that the effect of the proposed noise reduction method on the efficiency is small enough to be negligible at the rated power.

V. CONCLUSION

This paper experimentally assessed spread spectrum methods to reduce the radiation noise from the IPT system considering the misalignment of the coils. By randomly changing the transmission frequency of the inverter at random, the radiation emission was spread in the frequency domain. The output frequency was selected from the biased probability distribution considering the frequency dependence of the impedance. In this paper, two new biased distribution based on the input impedance were proposed in addition to the conventional method, which determined the biased distribution based on the combined impedance of the inductor and the compensation capacitor. The noise reduction effect was experimentally assessed. One of the proposed methods with the biased probability distribution, which was in proportion to the input impedance Z_{in}, provide the highest effect on the noise suppression on the fundamental and low-order harmonic components with or without the coil misalignment. The peak of the radiation noise measured at 0.5 m from the coil is suppressed from 52.9 dBμA to 39.5 dBμA. The proposed method is also effective even if the misalignment of the coils occurred. Moreover, the decrease of the maximum efficiency is smaller than the conventional spread spectrum method.

REFERENCES

[1] S. Y. R. Hui, W. Zhong, C. K. Lee: "A Critical Review of Recent Progress in Mid-Range Wireless Power Transfer", IEEE Trans. On Power Electronics, Vol. 29, No. 9, pp. 4500-4511 (2014)

[2] S. Li, C. C. Mi: "Wireless Power Transfer for Electric Vehicle Applications", IEEE Journal of Emerging and Selected Topics in Power Electronics, Vol. 3, No. 1, pp. 4-17 (2015)

[3] D. Shimode, T. Murai, S. Fujiwara, "A Study of Structure of Inductive Power Transfer Coil for Railway Vehicles", IEEJ Journal of Industry Applications, Vol. 4, No. 5, pp. 550-558 (2015).

[4] R. Ota, N. Hoshi, and J. Haruna, "Design of Compensation Capacitor in S/P Topology of Inductive Power Transfer System with Buck or Boost Converter on Secondary Side", IEEJ Journal of Industry Applications, Vol. 4, No. 4, pp. 476-485 (2015)

[5] H. Ishida, H. Furukawa, T. Kyoden, "Development of Design Methodology for 60Hz Wireless Power Transmission System", IEEJ Journal of Industry Applications, Vol. 5, No. 6, pp. 429–438 (2016)

[6] K. Kusaka, K. Orikawa, J. Itoh, I. Hasegawa, K. Morita, T. Kondo, "Galvanic Isolation System with Wireless Power Transfer for Multiple Gate Driver Supplies of a Medium-voltage Inverter," IEEJ Journal of Industry Applications, Vol. 5, No. 3, pp. 206–214 (2016)

[7] N. K. Trung, T. Ogata, S. Tanaka, K. Akatsu, "Analysis and PCB Design of Class D Inverter for Wireless Power Transfer Systems Operating at 13.56MHz", IEEJ Journal of Industry Applications, Vol. 4, No. 6, pp. 703-713 (2015)

[8] M. Jo, Y. Sato, Y. Kaneko, S. Abe: "Methods for Reducing Leakage Electric Field of a Wireless Power Transfer System for Electric Vehicles", IEEE Energy Conversion Congress and Exposition (ECCE) 2014, pp.1762-1769 (2014)

[9] H. Kim, J. Cho, S. Ahn, J. Kim, J. Kim: "Suppression of Leakage Magnetic Field from a Wireless Power Transfer System using Ferrimagnetic Material and Metallic Shielding", IEEE International Symposium on EMC, 978-1-4673-2061-0, pp.640-645 (2012)

[10] T. Campi, S. Cruciani, M. Feliziani: "Magnetic Shielding of Wireless Power Transfer Systems", IEEE International Symposium on EMC, 15A-H1, pp.422-425 (2014)

[11] K. Maikawa, K. Imai, Y. Minagawa, M. Arimitsu, H. Iwao: "Magnetic Field Reduction Technology of Wireless Charging System", in Proceedings, Society of Automotive Engineers of Japan 2013, No. 110-13 (2013)

[12] T. Shijo, K. Ogawa, M. Suzuki, Y. Kanekiyo, M. Ishida, S. Obayashi, "EMI Reduction Technology in 85 kHz Band 44 kW Wireless Power Transfer System for Rapid Contactless Charging of Electric Bus", IEEE Energy Conversion Congress & Expo 2016, No. EC-0641 (2016)

[13] K. Inoue, K. Kusaka, J. Itoh, "Reduction on radiation noise level for inductive power transfer systems with spread spectrum focusing on combined impedance of coils and capacitors," IEEE Energy Conversion Congress and Exposition (ECCE) 2016, pp. 1-8 (2016)

[14] K. Inoue, K. Kusaka, J. Itoh, "Reduction in Radiation Noise Level for Inductive Power Transfer Systems using Spread Spectrum Techniques," IEEE Trans. on Power Electronics, Vol. PP, No. 99, pp. 1-1 (2017)

[15] CISPR 11: 2015, "Industrial, scientific and medical equipment – Radio-frequency disturbance characteristics – Limits and methods of measurement (2015)

[16] Ministry of Internal Affairs and Communications, Japan, "Inquiry of technical requirements for wireless power transfer system for EVs in technical requirements for wireless power transfer system in standards of International Special Committee on Radio Interference (CISPR)", No. 3 (2015) (in Japanese)

[17] Y. H. Sohn, B. H. Choi, E. S. Lee, G. C. Lim, G. Cho, C. T. Rim: "General Unified Analyses of Two-Capacitor Inductive Power Transfer Systems: Equivalence of Current-Source SS and SP Compensations", IEEE Trans. On Power Electronics, Vol. 30, No. 11, pp. 6030-6045 (2015)

[18] R. Bosshard, J. W. Kolar, J. Muhlethaler, I. Stevanovic, B. Wunsch, F. Canales: "Modeling and eta-alpha-Pareto Optimization of Inductive Power Transfer Coils for Electric Vehicles", IEEE Journal of Emerging and Selected Topics in Power Electronics, Vol. 3, No. 1, pp. 50-64 (2015)

[19] R. L. Steigerwald, "A Comparison of Half-Bridge Resonant Converter Topologies," IEEE Trans. on Power Electronics Vol. 3, No. 2, pp. 174-182 (1992)

[20] K. Kim, Y. Jung, Y. Lim, "A New Hybrid Random PWM Scheme," IEEE Trans. on Power Electronics, Vol. 24, No. 1. pp. 192- 200 (2009)

[21] F. J. MacWilliams, N. J. A. Sloane, "Pseudo-random sequences and arrays," Proceedings of the IEEE, Vol. 64, No. 12, pp. 1715-1729 (1976)